Pedestrian-Induced Vibrations of Footbridges: An Extended Spectral Approach

K. Van Nimmen[1]; P. Van den Broeck[2]; G. Lombaert[3]; and F. Tubino[4]

Abstract: The vibration serviceability assessment of footbridges under pedestrian traffic requires a probabilistic approach considering the uncertainty in the dynamic behavior of the structure and the variability of multiple load parameters, such as the pedestrians' arrival time and step frequency. In view of engineering applications, a major challenge lies in the development, verification, and validation of efficient prediction models. With this challenge in mind, this paper uses a spectral approach to predict the dynamic response induced by unrestricted pedestrian traffic. A spectral load model available in the literature is extended to account for multiple harmonics of the vertical walking load and for application to arbitrary mode shapes. Furthermore, a closed-form expression is proposed to estimate the variance of the multimode structural response taking into account both resonant and nonresonant contributions. The performance of the proposed approach is evaluated for a simply supported beam as well as a real footbridge where multiple modes considerably contribute to the overall structural response. The results show that the proposed approach allows a good and mildly conservative estimate of the structural response to be obtained. **DOI: 10.1061/(ASCE)BE.1943-5592.0001582**.

Author keywords: Human-induced vibrations; Footbridge; Vibration serviceability; Spectral approach.

Introduction

In civil engineering, the increasing strength of new materials, the economic demand of efficiency, and esthetic requirements stimulate the design of lightweight, slender, and, consequently, vibration-sensitive structures (Ney and Poulissen 2014). When the structure is designed for human occupants (e.g., grandstands, footbridges, etc.), this trend is further stimulated by the relatively small service loads involved (Živanović et al. 2005; Smith et al. 2009; Heinemeyer et al. 2009b). For these structures, the vibration serviceability under human-induced loading has become a key design criterion when determining the structural shape and dimensions. Apart from a reliable description of the dynamic behavior of the structure, anticipating and preventing vibration serviceability failures requires reliable and detailed characterization of human dynamic actions (Racić et al. 2009; McDonald and Živanović 2017). Since the "wobbly" London Millennium Bridge brought this very problem in the limelight nearly two decades ago (Dallard et al. 2001), an extensive amount of research has been carried out on dynamic walking excitation. Significant progress has been made on the characterization of the intrinsic variability in the load pattern of an individual (Živanović et al. 2007; Racić and Brownjohn 2011) and the population (Sahnaci and Kasperski 2005; Piccardo and Tubino 2012), and the related human–structure interaction (HSI) (Agu and Kasperski 2011; Ingólfsson et al. 2012; Caprani and Ahmadi 2016; Shahabpoor et al. 2016b; Cappellini et al. 2016; Van Nimmen et al. 2017) and human–human interaction (HHI) (Bruno et al. 2011, 2016) phenomena. Furthermore, although the procedures presented by current guidelines focus on the resonant footbridge response (AFGC 2006; Heinemeyer et al. 2009a), recent observations indicate that also nonresonant contributions can be of significant importance to the overall dynamic performance (Dey et al. 2016).

Since the last decade, there exists a general consensus that the modeling of pedestrian traffic requires a probabilistic approach considering the variability of multiple load parameters such as the pedestrians' arrival time and step frequency (Živanović et al. 2007; Pedersen and Frier 2010; Krenk 2012; Piccardo and Tubino 2012; Demartino et al. 2017). A distinction is made between *interperson* and *intraperson* variability. Interperson variability refers to the fact that each pedestrian has their own characteristics, such as weight, step frequency, and walking speed (Caprani et al. 2012). In turn, intraperson variability refers to the fact that some parameters such as the step length and the walking speed may vary along the individual trajectories (Racić et al. 2009; Sahnaci and Kasperski 2011). In addition, the pedestrian's behavior is subject to various environmental stimuli such as the behavior of their neighbors and the group as a whole (HHI) (Helbing and Molnar 1995; Bruno and Venuti 2009; Bruno and Corbetta 2017), as well as the motion of the supporting structure (HSI) (Bocian et al. 2012; Carroll et al. 2012).

The method generally used to account for the probabilistic nature of pedestrian excitation is Monte Carlo (MC) simulation. Using MC simulation, the aim is to statistically characterize the (maximum) dynamic response of the footbridge for the considered loading conditions (Živanović et al. 2010; Van Nimmen et al. 2016). To this end, the structural response is evaluated for a large set of samples representing the desired traffic conditions, including the relevant HHI and HSI phenomena, and by sampling the involved load parameters from the proper probability distributions.

[1]Dept. of Civil Engineering, Structural Mechanics, KU Leuven, B-3001 Leuven, Belgium (corresponding author). ORCID: https://orcid.org/0000-0002-8188-1297. Email: katrien.vannimmen@kuleuven.be

[2]Dept. of Civil Engineering, TC Construction, Structural Mechanics, KU Leuven, B-9000 Ghent, Belgium. Email: peter.vandenbroeck@kuleuven.be

[3]Dept. of Civil Engineering, Structural Mechanics, KU Leuven, B-3001 Leuven, Belgium. Email: geert.lombaert@kuleuven.be

[4]DICCA, Univ. of Genoa, Via Montallegro 1, 16145, Genova, Italy. Email: federica.tubino@unige.it

Note. This manuscript was submitted on March 18, 2019; approved on February 19, 2020; published online on June 8, 2020. Discussion period open until November 8, 2020; separate discussions must be submitted for individual papers. This paper is part of the ***Journal of Bridge Engineering***, © ASCE, ISSN 1084-0702.

As these MC simulations are computationally expensive and not practical from the viewpoint of engineering applications, they are mainly used to derive and validate simplified procedures and spectral approaches.

- Simplified procedures aim to simulate, in an approximate way, the excitation by groups or crowds of pedestrians. The most widely applied approach involves the definition of an equivalent uniformly distributed resonant load producing the maximum dynamic response corresponding to a certain probability of exceedance (AFGC 2006; Heinemeyer et al. 2009a; BSI 2008). These approaches are generally overconservative, in particular for group loading, and do not allow to account for the contribution of multiple harmonics and modes, nor for nonresonant contributions (Živanović et al. 2005; Piccardo and Tubino 2012).
- In a spectral approach, the pedestrian-induced loading is modeled as a stationary random process by means of a suitable power spectral density (PSD) function (Ferrarotti and Tubino 2016). This approach was first introduced by Brownjohn et al. (2004) based on the probabilistic Gaussian distribution of step frequencies. Pizzimenti and Ricciardelli (2005) and Ricciardelli and Pizzimenti (2007) derived PSD functions for the lateral component of the single-person walking load. Caprani (2014) proposed a spectral model to encompass both intrapedestrian and interpedestrian variability. A wide experimental campaign has been carried out recently to provide a more reliable spectral characterization of the vertical component of the walking load, providing parameters for the first six harmonics (Chen et al. 2019). A different model has been proposed by Casciati et al. (2017), with a mathematical form similar to that used in wind engineering. Starting from these spectral models, the dynamic response can be estimated based on time-domain numerical simulations of the loading (Caprani 2014; Casciati et al. 2017), or on frequency-domain numerical evaluations of the spectral moments (Bassoli et al. 2018). Based on a spectral representation of the loading, other authors have focused on the search for closed-form expressions for the dynamic response to walking. Krenk (2012) introduced simplified expressions for the standard deviation of the structural response of a single-degree-of-freedom (SDOF) system to (resonant and nonresonant) excitation with a frequency distribution representative for the fundamental harmonic of the walking load. An equivalent spectral model for the walking load in unrestricted pedestrian traffic condition has been deduced analytically, verified numerically, and validated experimentally by Piccardo and Tubino (2012) and Tubino et al. (2016). Piccardo and Tubino (2012) proposed a closed-form expression for the variance and the maximum value of the structural response to unrestricted pedestrian traffic due to the fundamental harmonic of the walking load and considering only the resonant contribution of a bending mode of a footbridge. This spectral approach has been shown to provide excellent results when the structural response is dominated by the contribution of a single mode when the mean value of the step frequencies is (very) close to its natural frequency.

The limitations and assumptions related to the closed-form solution for the dynamic response proposed in Piccardo and Tubino (2012) are as follows.

- It accounts only for the contribution of a single mode and a single harmonic. A generalization to multiharmonic response using the square root of the sum of the squares (SRSS) combination rule was proposed by Bassoli et al. (2018), but the maximum single-mode structural acceleration due to a single harmonic of the walking load is estimated numerically.
- It can only be applied to purely bending modes.
- Focus is only on the vertical component of the walking load.
- Unrestricted traffic conditions are considered whereby the walking trajectories can be approximated by straight lines. This assumption can be made for bridge decks with a constant width and low pedestrian densities (up to 0.5 pedestrians/m^2 Weidmann 1993; Venuti and Bruno 2007; Ferrarotti and Tubino 2016), where the walking behavior of the pedestrians is not (or is only negligibly) influenced by HHI and the interperson variability in step frequency can be described by a Gaussian distribution, as also assumed by Bassoli et al. (2018), Krenk (2012), and Piccardo and Tubino (2012). Preliminary results (Wei et al. 2017), however, also suggest that the effect of social forces (Helbing et al. 2000), including HHI, on the dynamic structural response can be accounted for by straight walking trajectories and an equivalent distribution of step frequencies. To account for HHI in the spectral model, a possible extension of the model was discussed in Ferrarotti and Tubino (2016). Microscopic modeling of pedestrian traffic is outside the scope of this paper, but the reader is referred to Bruno and Corbetta (2017), Bruno et al. (2011), Helbing et al. (2000), and Venuti et al. (2016) for more information on this topic.
- *Active* HSI phenomena are disregarded: *active* interaction phenomena, whereby the walking behavior of the pedestrian is modified in response to the vibration of the surface, are known to occur for lateral bridge deck motion (Ingólfsson et al. 2012; Erlicher et al. 2010; Carroll et al. 2014; Fujino and Siringoringo 2015; Bocian et al. 2016). In the vertical direction, it is argued that they are only achieved for vibration amplitudes that exceed the acceptable limits for vibration comfort (AFGC 2006; Butz et al. 2008; Dang and Živanović 2016).

This paper extends the spectral approach proposed by Piccardo and Tubino (2012) and adopted by Bassoli et al. (2018) as follows.

- It is generalized analytically for multiharmonic excitation.
- It is generalized analytically for the multimode dynamic response of footbridges with widely spaced modes. This limitation is met by the majority of footbridges.
- It is extended for application to arbitrary mode shapes, e.g., for cases where also the distribution of pedestrians along the width of the bridge deck is of importance due to the presence of torsional modes.
- A closed-form expression is proposed to estimate the variance of the multimode structural response taking into account both resonant and nonresonant contributions.

Every step in the extension process is numerically verified using MC simulations, considering the variability of the relevant load parameters. First, the process is verified for a simply supported beam where only the fundamental mode is considered. This allows an evaluation of the performance of the spectral approach for a wide range of modal parameters, in particular, a wide range of natural frequencies and modal damping ratios. The considered range of damping ratios is significantly wider than what is generally considered for inherent structural damping with the aim of also encompassing the added damping due to passive HSI phenomena (Van Nimmen et al. 2017; Shahabpoor et al. 2016a; Sachse et al. 2004; Tubino 2018) or passive vibration mitigation measures (Weber and Feltrin 2010). The spectral approach presented in Bassoli et al. (2018) was the first to explicitly account for passive HSI, but the method proposed only allows numerical estimation of the single-mode structural response. The results are furthermore also compared with those obtained using the closed-form solution introduced by Krenk (2012). Second, the generalized spectral approach is verified through application to a real footbridge where multiple low-frequency modes contribute to the structural response.

The outline of this paper is as follows. First, the general mathematical framework for the calculation of the structural response to pedestrian traffic is presented. Second, the basic principles of

the spectral approach and its generalization to multiharmonic excitation and the estimation of a multimode structural response are discussed. Third, the proposed approach is verified numerically. Finally, conclusions are formulated.

Structural Response to Unrestricted Pedestrian Traffic

The equations of motion of a footbridge, modeled as a 2D continuous linear structural system with classical viscous damping, can be written in the following form:

$$\mathcal{M}(x, y)\frac{\partial^2 u(x, y; t)}{\partial^2 t} + \mathcal{C}\left[\frac{\partial u(x, y; t)}{\partial t}\right] + \mathcal{L}\left[u(x, y; t)\right] = f(x, y; t) \tag{1}$$

where $u(x, y; t)$ = displacement of the footbridge; t (s) = time; x and y (m) = abscissa along the longitudinal and the lateral axis of the structure with dimensions l_x and l_y (m), respectively; $\mathcal{M}(x, y)$ = structural mass per unit area; $\mathcal{C}$ and $\mathcal{L}$ = damping and stiffness operator, respectively; and $f(x, y; t)$ = external force.

The external force in this study consists of the vertical pedestrian excitation, which can be expressed as the sum of moving multiharmonic loads:

$$f(x, y; t) = \sum_{h=1}^{m_h}\sum_{p=1}^{m_p} \alpha_{hp} G_p \sin\left(h\omega_{sp}t + \vartheta_h + \vartheta_p\right)\delta\left[x - \bar{v}_s(t - \tau_p)\right] \times \delta\left[y - y_p\right]\left[\mathbb{H}(t - \tau_p) - \mathbb{H}\left(t - \tau_p - \frac{l_x}{\bar{v}_s}\right)\right] \tag{2}$$

where α_{hp} (-) = dynamic load factor (DLF); G_p (N) = the weight; ω_{sp} (rad/s) = circular step frequency; ϑ_p (rad) = phase angle; τ_p (s) = arrival time; y_p (m) = abscissa along the width of the bridge deck of the pth pedestrian; h = order number of the harmonic; m_h = number of harmonics; m_p = number of pedestrians; ϑ_h (rad) = phase angle of the hth harmonic; $\bar{v}_s$ = average walking speed of the pedestrians; $\delta(\cdot)$ = Dirac function; and $\mathbb{H}(\cdot)$ = Heaviside function. The phase angle ϑ_p and the position of the pedestrians along the width y_p are assumed to be random variables, distributed uniformly in $[0, 2\pi]$ and $[0, l_y]$, respectively. The arrival times are assumed to follow a Poisson distribution (Helbing and Molnar 1995; Živanović 2012).

After applying the modal coordinate transformation,

$$u(x, y, t) = \sum_{j=1}^{m_m} \phi_j(x, y) z_j(t) \tag{3}$$

where ϕ_j = jth unity-normalized mode shape; and m_m = number of modes and assuming proportional damping; the equation of motion of the jth modal coordinate z_j can be expressed as

$$\ddot{z}_j(t) + 2\xi_j\omega_j\dot{z}_j(t) + \omega_j^2 z_j(t) = \frac{1}{m_j} f_j(t) \tag{4}$$

where ξ_j (-) =jth modal damping ratio; ω_j (rad/s) = natural circular frequency; $n_j = \omega_j/2\pi$ (Hz) = natural frequency; m_j = modal mass; and $f_j(t)$ is the jth modal load given by

$$f_j(t) = \sum_{h=1}^{m_h}\sum_{p=1}^{m_p} \alpha_{hp} G_p \sin\left(h\omega_{sp}t + \vartheta_h + \vartheta_p\right)\phi_j'\left[\bar{v}_s(t - \tau_p), y_p\right] \tag{5}$$

with $\phi_j' = \phi_j$ for $0 \le \bar{v}_s(t - \tau_p) \le l_x$ and $\phi_j' = 0$ otherwise. When the step frequency, or one of its multiples, coincides with the jth natural frequency of the footbridge, and when it is assumed that the structural response is dominated by the resonant contribution of that mode, Eqs. (3) and (5) are often reduced to the contribution of the resonant mode j and the resonant harmonic h only.

Spectral Approach

This section first discusses the spectral approach for the special case of single-harmonic excitation and the estimation of the single-mode resonant structural response (section "Single-Harmonic Excitation, Single-Mode Response"). The formulations presented in this section are borrowed and adapted from Ferrarotti and Tubino (2016), Krenk (2012), and Piccardo and Tubino (2012). Section "Multiharmonic Excitation, Multimode Response" then discusses the generalization of the spectral approach for the application to multiharmonic excitation and the estimation of a multimode structural response.

Single-Harmonic Excitation, Single-Mode Response

The spectral approach introduced by Piccardo and Tubino (2012) only considers vertical bending modes, making the pedestrians' location along the lateral dimension of the footbridge y nonessential. Then, when only the fundamental harmonic of the walking load is accounted for ($h = 1$), the modal force in Eq. (5) reads (Piccardo and Tubino 2012)

$$f_j(t) \cong \sum_{p=1}^{m_p} \alpha_{1p} G_p \sin\left(\omega_{sp}t + \vartheta_p\right)\phi_j'\left(\bar{v}_s t - \tau_p\right) \tag{6}$$

Given that the time needed by the pedestrian to cross the length corresponding to a single sine wave of the structural mode ϕ_j is much longer than the period of the force, the last term in Eq. (6), $\phi_j(\bar{v}_s t - \tau_p)$, can be interpreted as a *window* function (Bendat and Piersol 2010) as considered in the spectral analysis of random processes (Elishakoff 1999; Bendat and Piersol 2010). Following these developments, the single-sided PSD function of the modal force $S_{f_j}(\omega)$ induced by m_p pedestrians is found as (Piccardo and Tubino 2012)

$$S_{f_j}(\omega) = \frac{m_p \bar{\alpha}_1^2 \bar{G}^2}{2} p_{\omega_s}(\omega)\left[\frac{1}{l_x}\int_0^{l_x} \phi_j^2(x)\,\mathrm{d}x\right] \tag{7}$$

with $p_{\omega_s}(\omega)$ the probability density function (PDF) of the step frequency ω_{sp}.

To arrive at Eq. (7), a number of simplifying assumptions are made regarding interperson and intraperson variability. Tubino and Piccardo (2016) showed that the interperson variability of the walking speed, the pedestrian weight, and the DLFs have a negligible influence on the structural dynamic response (Tubino and Piccardo 2016). Therefore, these quantities are modeled deterministically through their mean value. As a result, only the variability of the step frequency is considered, that is, the load parameter that predominantly governs the structural response (Van Nimmen et al. 2014; Tubino and Piccardo 2016; McDonald and Živanović 2017). Van Nimmen et al. (2017) showed that for a considerable degree of interperson variability, as typically associated with unrestricted traffic conditions, the effect of interperson variability on the structural dynamic response prevails over that of intraperson variability. In other words, Van Nimmen et al. (2017) showed that considering the step frequency ω_s as a random variable, characterized by a probability distribution function (PDF) describing the interperson variability of unrestricted traffic, is representative for the dynamic effect of both interperson and intraperson variabilities in step frequency. Based on the results reported in the literature (Racić et al. 2009; Pedersen and Frier 2010), a Gaussian distribution of step frequencies

is assumed. The PDF $p_{\omega_s}(\omega)$ then reads

$$p_{\omega_s}(\omega) = \frac{1}{\sigma_{\omega_s}\sqrt{2\pi}} e^{-(\omega-\bar{\omega}_s)^2/2\sigma_{\omega_s}^2} \tag{8}$$

where $\bar{\omega}_s$ = mean value of the circular step frequencies; and σ_{ω_s} = standard deviation of the circular step frequencies.

Based on the analytical spectral model of the modal force, Eq. (7), the PSD function of the modal accelerations is given by

$$S_{\ddot{z}_j}(\omega) = \left|H_{\ddot{z}_j}(\omega)\right|^2 S_{f_j}(\omega) \tag{9}$$

where $H_{\ddot{z}_j}(\omega)$ = complex frequency response function (FRF) of the jth modal coordinate in terms of accelerations. By assuming that the response of footbridges is mainly resonant, the variance of $\ddot{z}_j$ can be estimated through the classical methods of random vibration for linear problems (Elishakoff 1999):

$$\sigma_{\ddot{z}_j}^2 = \frac{\pi\omega_j}{4m_j^2\xi_j} S_{f_j}(\omega_j) \tag{10}$$

with $S_{f_j}(\omega_j)$ the single-sided PSD function of the modal force, Eq. (7), evaluated for $\omega = \omega_j$.

In addition, Krenk (2012) introduced a closed-form expression for the standard deviation of the response of a SDOF system excited by a force characterized by a Gaussian frequency distribution. In the context of the present paper, the proposed expression is written as follows:

$$\sigma_{\ddot{z}_j} \cong \frac{\bar{\alpha}_1 \bar{G}\sqrt{m_p\sqrt{\pi}}}{4m_j^2\sqrt{\xi_j}} \frac{\sqrt{\xi_j+\xi_0}\left(1+\omega_0^2\right)}{\sqrt{\left(1-\omega_0^2\right)^2+4\left(\xi_j+\xi_0\right)^2\omega_0^2}} \tag{11}$$

$$\omega_0 = \frac{\bar{\omega}_s}{\omega_j}\sqrt{1+2cs^2}, \quad \xi_0 = c_s\sqrt{\frac{2}{1+2c_s^2}} \tag{12}$$

where $c_s = \sigma_{\omega_s}/\bar{\omega}_s$ = coefficient of variation (COV) of the step frequency. In contrast to Eqs. (10) and (11) also retains validity for nonresonant excitation.

By assuming that the structural response is dominated by the jth mode, the variance of the acceleration response in physical coordinates may finally be estimated as

$$\sigma_{\ddot{u}}^2(x) = \phi_j^2(x)\sigma_{\ddot{z}_j}^2 \tag{13}$$

where x = physical coordinate of the desired output location on the bridge deck.

Although used by most of the current guidelines, the peak acceleration response as a measure for footbridge vibration serviceability has been called into question (Tubino and Piccardo 2016). The reason for this is that it concerns an instantaneous quantity that is potentially not representative for the overall comfort evaluation, in particular when the structural response results from relevant resonant and nonresonant (transient) contributions, whether or not from multiple structural modes. Furthermore, for spectral approaches, maximum acceleration levels can be estimated through the application of a suitable peak factor (Davenport 1964), which involves additional assumptions and approximations that are not to the benefit of the accuracy of the obtained result. On the other hand, the variance or standard deviation of the dynamic response can be estimated accurately (Tubino and Piccardo 2016). It is for this reason that this study evaluates the structural acceleration response in terms of its standard deviation $\sigma_{\ddot{u}}(x)$.

Multiharmonic Excitation, Multimode Response

In reality, the dynamic walking load is composed of multiple harmonics m_h. Consequently, the loading due to m_p pedestrians can be considered as a narrow-band random process characterized by dominant contributions around $h\omega_h$ with $h \in \mathbb{N}$ [Eq. (2) and Fig. 1-top]. To account for the multiple harmonics m_h in the walking load, the modal force in Eq. (6) is reformulated as

$$f_j(t) \cong \sum_{h=1}^{m_h}\sum_{p=1}^{m_p} \alpha_{hp} G_p \sin\left(h\omega_{sp}t + \vartheta_p + \vartheta_h\right)\phi_j'\left(\bar{v}_s t - \tau_p, y_p\right) \tag{14}$$

where $h\omega_{sp}$ = hth harmonic of the step frequency for which the PDF $p_{h\omega_s}(\omega)$ is found as

$$p_{h\omega_s}(\omega) = \frac{1}{h\sigma_{\omega_s}\sqrt{2\pi}} e^{-(\omega-\omega_h)^2/2(h\sigma_{\omega_s})^2} \tag{15}$$

where $\omega_h = h\bar{\omega}_s$ = mean value of the hth harmonic; and $h\sigma_{\omega_s}$ = standard deviation of the hth harmonic. Similar to Eq. (6), $\phi_j(\bar{v}_s t - \tau_p, y_p)$ can be interpreted as a window function. In addition, accounting for the phases of the different harmonics that are independent and uniformly distributed (Živanović et al. 2007), their contributions are uncorrelated and the single-sided PSD function of the modal load reads (Elishakoff 1999)

$$\begin{aligned} S_{f_j}(\omega) &= \sum_{h=1}^{m_h} S_{f_{j,h}}(\omega) \\ &= \sum_{h=1}^{m_h} \frac{m_p\bar{\alpha}_h^2\bar{G}^2}{2} p_{h\omega_s}(\omega)\left[\frac{1}{l_x l_y}\int_0^{l_x}\int_0^{l_y}\phi_j^2(x,y)\,\mathrm{d}x\,\mathrm{d}y\right] \end{aligned} \tag{16}$$

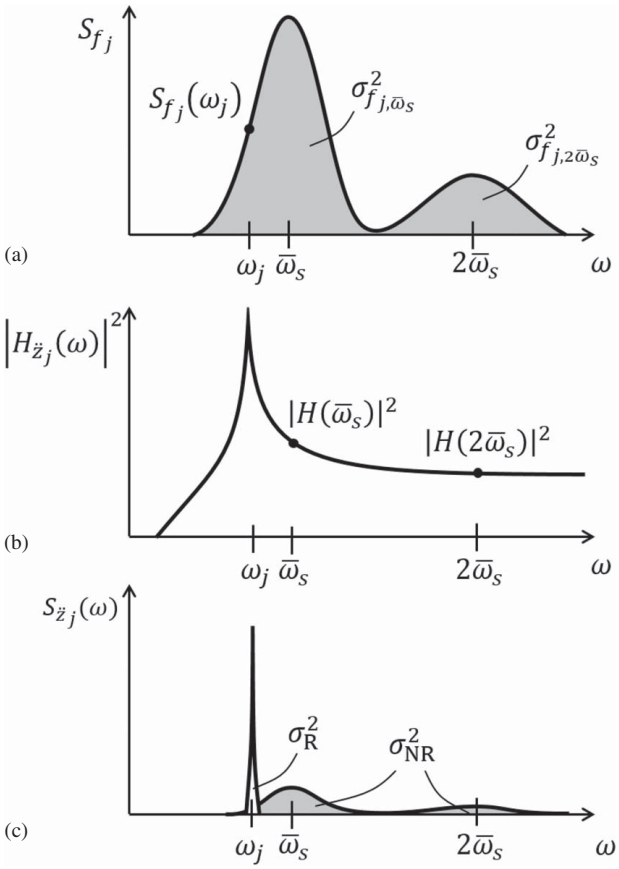

Fig. 1. (a) Schematic representation of a multiple narrow-band random process; (b) the FRF of a SDOF system in modal coordinates; and (c) the resulting modal acceleration response.

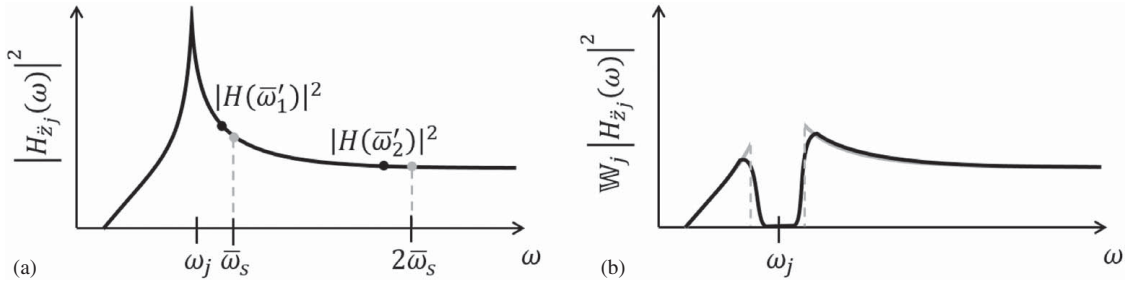

Fig. 2. Schematic illustration of the corrections described by (a) Eq. (23); and (b) Eq. (26).

where $S_{f_{j,h}}(\omega)$ = PSD function of the modal load associated with the hth harmonic. Eq. (16) [and Eq. (7)] are valid for low values of the COV of α_h G. However, the higher harmonics of the walking load are known to be characterized by higher values for the COV (≈0.40), in comparison with that of the fundamental harmonic (≈0.17) (Willford and Young 2006). To also account for larger values of the COV for the different harmonics, the property for the variance of products (Goodman 1960) is used to further extend Eq. (16) to

$$S_{f_j}(\omega) = \sum_{h=1}^{m_h} \frac{m_p \bar{\alpha}_h^2 \bar{G}^2 (1 + c_h^2)}{2} p_{h\omega_s}(\omega) \left[\frac{1}{l_x l_y} \int_0^{l_x} \int_0^{l_y} \phi_j^2(x, y) \, \mathrm{d}x \, \mathrm{d}y \right] \quad (17)$$

where c_h = COV of $\alpha_h G$, with $\alpha_h G$ and $p_{h\omega_s}$ as independent random variables. It is noted that in Eq. (17), $\alpha_h G$ is considered as a single random variable. In case the random variables α_h and G are individually statistically characterized and they are statistically independent, the COV of their product can be estimated from the COV of the single variables (c_{α_h} and c_G) as $c_h = \sqrt{c_{\alpha_h}^2 + c_G^2 + c_{\alpha_h}^2 c_G^2}$.

The variance of $\ddot{z}_j$ is now given by

$$\sigma_{\ddot{z}_j}^2 = \int_0^\infty |H_{\ddot{z}_j}(\omega)|^2 S_{f_j}(\omega) \, \mathrm{d}\omega = \sum_{h=1}^{m_h} \int_0^\infty |H_{\ddot{z}_j}(\omega)|^2 S_{f_{j,h}}(\omega) \, \mathrm{d}\omega \quad (18)$$

The variance of the response can be considered as the superposition of a resonant and a nonresonant contribution [see Fig. 1(c)]:

$$\sigma_{\ddot{z}_j}^2 = \sigma_{\ddot{z}_{j,r}}^2 + \sigma_{\ddot{z}_{j,nr}}^2 \quad (19)$$

with

$$\sigma_{\ddot{z}_{j,r}}^2 = \int_{\omega_j - \varepsilon}^{\omega_j + \varepsilon} |H_{z_j}(\omega)|^2 S_{f_j}(\omega) \, \mathrm{d}\omega \cong S_{f_j}(\omega_j) \int_{\omega_j - \varepsilon}^{\omega_j + \varepsilon} |H_{z_j}(\omega)|^2 \mathrm{d}\omega \cong \frac{\pi \omega_j}{4 m_j^2 \xi_j} S_{f_j}(\omega_j) \quad (20)$$

$$\sigma_{\ddot{z}_{j,nr}}^2 = \sum_{h=1}^{m_h} \int_0^{\omega_j - \varepsilon} |H_{\ddot{z}_j}(\omega)|^2 S_{f_{j,h}}(\omega) \, \mathrm{d}\omega + \int_{\omega_j + \varepsilon}^\infty |H_{\ddot{z}_j}(\omega)|^2 S_{f_{j,h}}(\omega) \, \mathrm{d}\omega \quad (21)$$

where ε is a small parameter. When the dominant peak of the PSD function of the hth harmonic $S_{f_{j,h}}$ is sufficiently narrow, or when the FRF $H_{\ddot{z}_j}(\omega)$ is approximately constant around ω_h, then Eq. (21) can be approximated by

$$\sigma_{\ddot{z}_{j,nr}}^2 = \sum_{h=1}^{m_h} \sigma_{f_{j,h}}^2 |H_{\ddot{z}_j}(\omega_h)|^2 \left(1 + \mathbb{H}[\omega_j - \varepsilon - \omega_h] - \mathbb{H}[\omega_j + \varepsilon - \omega_h] \right) \quad (22)$$

where $\sigma_{f_{j,h}}^2 = \int_0^\infty S_{f_{j,h}}(\omega) \, \mathrm{d}\omega$ = variance of the hth harmonic of the jth modal load. The Heaviside function in Eq. (22) enforces that the nonresonant response is only accounted for when $\omega_h \notin [\omega_j - \varepsilon; \omega_j + \varepsilon]$.

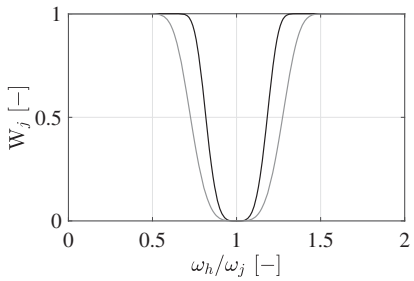

Fig. 3. The function $\mathbb{W}_j(\omega_h)$ as proposed as a smooth alternative for the Heaviside function $\mathbb{H}$, for the fundamental (black) and second (gray) harmonic of the walking load.

The following two corrections are now proposed.

- As $|H_{\ddot{z}_j}(\omega)|$ is increasing towards ω_j, assuming that $H_{\ddot{z}_j}(\omega)$ is constant for the relevant width of the peak in $S_{f_{j,h}}$ [$H_{\ddot{z}_j}(\omega) = H_{\ddot{z}_j}(\omega_h)$], can result in an underestimation of the nonresonant response. To address this issue, Eq. (22) is modified as follows:

$$\sigma_{\ddot{z}_{j,nr}}^2 = \sum_{h=1}^{m_h} \sigma_{f_{j,h}}^2 |H_{\ddot{z}_j}(\omega_h')|^2 \left(1 + \mathbb{H}[\omega_j - \varepsilon - \omega_h] - \mathbb{H}[\omega_j + \varepsilon - \omega_h] \right) \quad (23)$$

with $\omega_h' = (1 - \varsigma)\omega_h + \varsigma \omega_j$ with $\varsigma \geq 0$ and $\varsigma \ll 1$ [see also Fig. 2(a)]. This modification implies that Eq. (23) evaluates the FRF $H_{\ddot{z}_j}(\omega)$ at a frequency ω_h' that is $100 \times \varsigma$% closer to ω_j than ω_h, with $|H_{\ddot{z}_j}(\omega_h')| \geq |H_{\ddot{z}_j}(\omega_h)|$. A value of 0.2 is proposed for ς. The effect of this parameter is further illustrated in section "Numerical Verification: Single-Harmonic, Single-Mode."
- In reality, the influence of the nonresonant response gradually increases as ω_h moves further away from ω_j. To gradually account for the nonresonant response, the Heaviside function in Eqs. (22) and (23), can be replaced by a smooth approximation to the step function such as the logistic function or a Gaussian PDF-inspired function. Based on the latter, the function $\mathbb{W}_j(\omega_h)$ is proposed:

$$\mathbb{W}_j(\omega_h) = 1 - e^{-[(\omega_h - \omega_j)/a_1 \omega_j]^4} \quad (24)$$

Based on empirical numerical investigations, the following value is proposed for a_1:

$$a_1 = 0.1(1 + h) \quad (25)$$

The corresponding function $\mathbb{W}_j(\omega_h)$ is visualized in Fig. 3. The dependence on h in Eq. (25) is introduced to expand the interval around ω_j where the resonant contribution dominates the response [see also Figs. 2(b) and 3]. This is in line with the width of the dominant spectrum of the harmonic load that increases with h.

Eq. (23) then reads

$$\sigma^2_{\ddot{z}_{j,nr}} = \sum_{h=1}^{m_h} \sigma^2_{f_{j,h}} \left|H_{\ddot{z}_j}(\omega'_h)\right|^2 \mathbb{W}_j(\omega_h) \tag{26}$$

The effect of $\mathbb{W}_j$ is further illustrated in section "Numerical Verification: Single-Harmonic, Single-Mode."

When the modes are well separated (Chopra 1995), the modal dynamic responses may be assumed as uncorrelated and the standard deviation of the acceleration response is found following the SRSS rule for modal combination (Chopra 1995):

$$\sigma_{\ddot{u}}(x, y) = \sqrt{\sum_{j=1}^{m_m} \phi_j^2(x, y)\sigma^2_{\ddot{z}_j}} \tag{27}$$

with (x, y) the physical coordinate of the desired output location on the bridge deck. In case the modes cannot be considered as well separated, an alternative for SRSS is provided by the complete quadratic combination (CQC) modal combination rule that allows the correlation among the modal responses to be accounted for (Chopra 1995). In its current form, the proposed method does not provide the necessary inputs for the CQC method, therefore its application is limited to widely spaced modes. This limitation is met by the majority of footbridges.

Numerical Verification: Single-Harmonic, Single-Mode

To provide numerical verification of the proposed expressions for the PSD function of the modal load and the variance of the dynamic response, a simple case is considered first. This simple case corresponds to a footbridge with a length of $l_x = 100$ m and a width of $l_y = 3$ m. The mode shape ϕ_j corresponds to the fundamental mode of a simply supported beam, i.e., a half sine wave. The modal mass m_j is set to 50,000 kg. Different values are considered for the natural frequency ω_j and the modal damping ratio ξ_j, as discussed in the following paragraphs.

A pedestrian density of 0.5 persons/m^2 is considered, corresponding to a total of $m_p = 150$ pedestrians on the footbridge. Following the speed–density relation defined by Bruno and Venuti (2009), a mean walking speed $\bar{v}_s = 1.30$ m/s is found for a pedestrian density of 0.5 persons/m^2. The distribution of step frequencies is set to follow a Gaussian distribution $\omega_s = \mathcal{N}(\bar{\omega}_s, \sigma_{\omega_s})$ (rad/s). Different values are considered for the mean value of the step frequencies $\bar{\omega}_s$, as discussed next in the following paragraphs. In this section, only the fundamental harmonic of the walking load is considered: $\omega_h = \omega_s$. The standard deviation of the step frequencies is set to 0.18 Hz ($\sigma_{\omega_s} = 0.18 \times 2\pi$), which is representative for unrestricted traffic conditions (AFGC 2006). The amplitude of the harmonic walking load $\bar{\alpha}\bar{G}$ is set equal to 0.4×700, corresponding to the average value for the DLF of the fundamental harmonic of the walking load and pedestrian weight, respectively (AFGC 2006).

The standard deviation of the acceleration levels is evaluated for a wide range of ω_h/ω_j ($\omega_h/\omega_j \in [0.2, 4]$) and modal damping ratios ($\xi_j \in [0.5, 10.0]$%). Although the inherent structural damping ratios are usually (well) below 3% for footbridges, effective damping ratios up to 10% are considered here to also anticipate the effect of passive HSI (Van Nimmen et al. 2017).

For each case, the PSD function of the modal load and the standard deviation of the dynamic response is estimated (1) numerically based on a large number of $m_{\text{sim}} = 10^4$ MC simulations (following the mathematical framework described in section "Structural Response to Unrestricted Pedestrian Traffic") and (2) by the simplified expressions proposed in section "Spectral Approach": Eq. (7) for the modal load and Eqs. (27), (19), (20), and (26) for the estimation of the dynamic response.

PSD Function of the Modal Load

Considering a sinusoidal mode shape and a single harmonic, Eq. (17) becomes

$$S_{f_j}(\omega) = \frac{m_p \bar{\alpha}_1^2 \bar{G}^2 \left(1 + c_1^2\right)}{4} p_{\omega_s}(\omega) \tag{28}$$

The PSD function of the modal force is now verified for different values of the COV ($0 \le c_1 \le 0.4$), which is in this example fully attributed to the variability of α_1 (and, thus, assuming $G_p = \bar{G}$). Fig. 4 compares the PSD function of the modal load as analytically predicted using Eq. (28) to the PSD function of the modal load as derived from the numerical simulations. These results show that the influence of the COV of variation of α_h G is not negligible, especially in the range [1.7, 2.1] Hz [Fig. 4(b)]. The maximal value of the PSD function of the modal load for a COV equal to 0.4 is found to be 14% greater than for a COV equal to 0. Fig. 4 also shows that an excellent agreement is found between the analytical predictions and the numerical simulations. Small differences between the analytical predictions and the numerical simulations arise for larger values of the COV. These differences may result from the fact that the normal distributions are no longer perfectly normal as they are truncated to exclude negative nonphysical values of α_1. In the following sections, the COV of α_h G is set equal to zero.

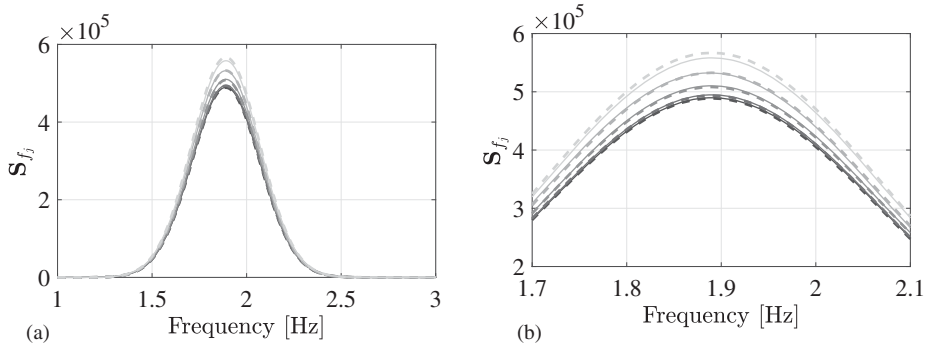

Fig. 4. PSD function of the modal force ($m_p = 150$) as analytically predicted (dashed) and numerically simulated (solid) for a COV c_1 of {0.0, 0.1, 0.2, 0.3, 0.4} (dark to light): (a) 1 Hz up to 3 Hz; and (b) zoom for 1.7 Hz up to 2.1 Hz.

Structural Dynamic Response

First, focus is on the PSD function of the structural accelerations for three distinguished values of $\omega_h = \{0.5, 1.0, 2.0\} \times \omega_j$. For these load cases, Fig. 5 shows the PSD function of the modal load together with the FRF of the footbridge, and the PSD of the resulting structural accelerations. From Fig. 5(e) it is clear that for $\omega_h = \omega_j$, the structural response is governed by the resonant contribution. For $\omega_h = 0.5\omega_j$ and $\omega_h = 2.0\omega_j$ the structural response is governed by the nonresonant contribution [Figs. 5(d and f)] and the shape of $S_{\ddot{u}}$ is similar to the shape of S_{f_j}. Since the FRF $H_{\ddot{z}_j}(\omega)$ is not perfectly flat around ω_h but increasing towards ω_j, the bell curve of S_{f_j} reflected in $S_{\ddot{u}}$ is skewed towards ω_j, which is more pronounced as ω_h is closer to ω_j.

Second, focus is on the standard deviation of the structural response. Fig. 6 compares the numerically simulated results with those predicted analytically first considering the resonant contribution only [$\sigma^2_{\ddot{z}_j} \approx \sigma^2_{\ddot{z}_{j,r}}$, Eq. (20)] and, next, considering both the resonant and nonresonant contribution [$\sigma^2_{\ddot{z}_j} \approx \sigma^2_{\ddot{z}_{j,r}} + \sigma^2_{\ddot{z}_{j,nr}}$, Eqs. (27), (19), (20), and (26)], and predicted according to Krenk (2012) [Eq. (11)]. When the numerical simulations are compared with the

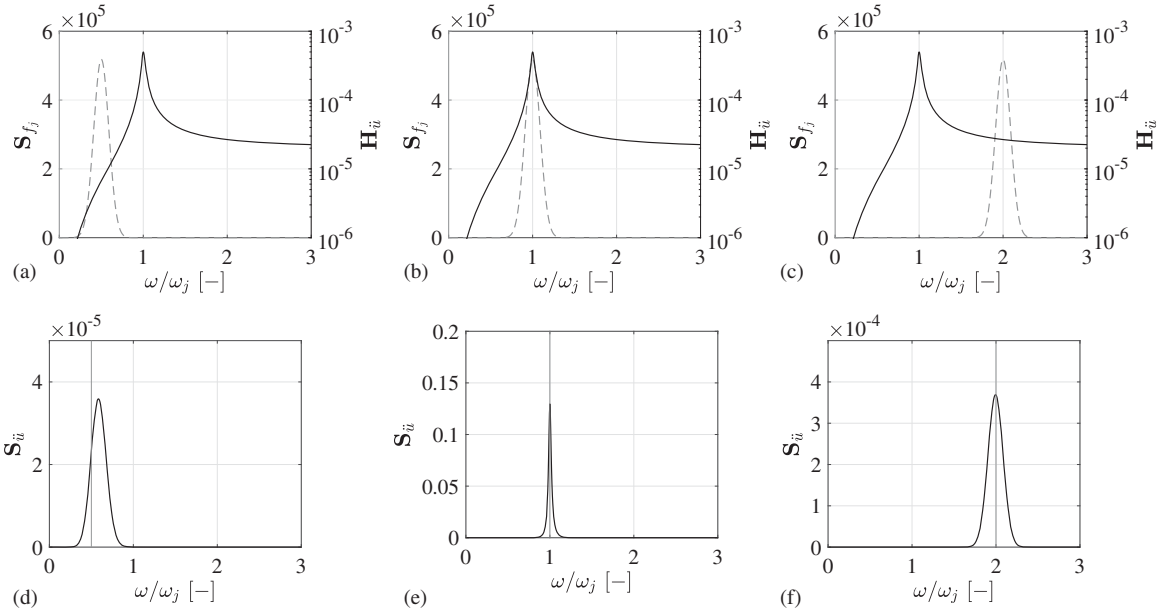

Fig. 5. For a pedestrian density of 0.5 pedestrians/m^2 and a modal damping ratio of $\xi_j = 2.0\%$, in terms of ω_h/ω_j: (top) the PSD of f_j (dashed) and the FRF of the footbridge (solid); and (bottom) the PSD of $\ddot{u}$, with (a and d) $\omega_h = 0.5\omega_j$, (b and e) $\omega_h = \omega_j$, and (c and f) $\omega_h = 2\omega_j$.

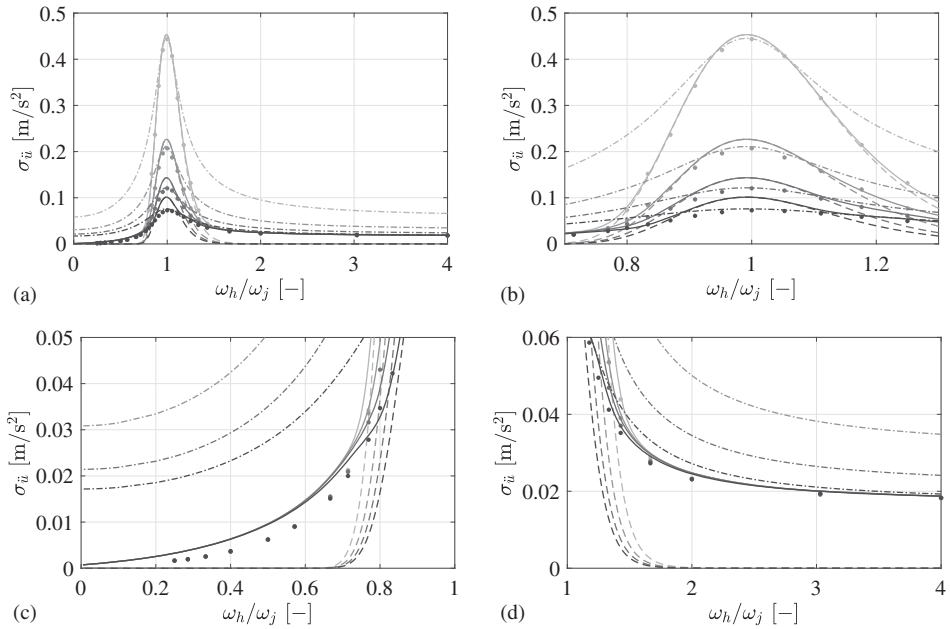

Fig. 6. Comparison between the analytically predicted (curve) and numerically simulated (•) standard deviation of $\ddot{u}$, in terms of ω_h/ω_j, for a pedestrian density of 0.5 pedestrians/m^2 and for different values of the modal damping ratio (light to dark) $\xi_j = \{0.5, 2.0, 5.0, 10.0\}\%$ according to $\sigma^2_{\ddot{z}_j} = \sigma^2_{\ddot{z}_{j,r}}$ (dashed) and $\sigma^2_{\ddot{z}_j} = \sigma^2_{\ddot{z}_{j,r}} + \sigma^2_{\ddot{z}_{j,nr}}$ (solid) and according to Krenk (Krenk 2012) [Eq. (11), dash-dotted]: (a) $0 \le \omega_h/\omega_j \le 4$; (b) zoom $0.7 \le \omega_h/\omega_j \le 1.3$; (c) $0 \le \omega_h/\omega_j \le 1$; and (d) zoom $1 \le \omega_h/\omega_j \le 4$.

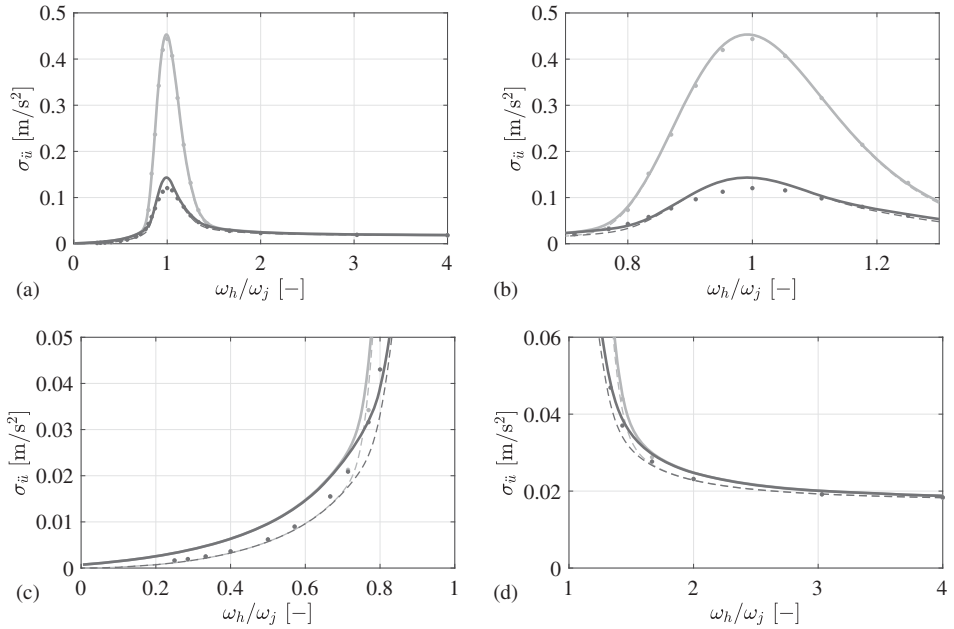

Fig. 7. Comparison between the analytically predicted (curve) and numerically simulated (•) standard deviation of $\ddot{u}$, in terms of ω_h/ω_j, for a pedestrian density of 0.5 pedestrians/m^2 and for a modal damping ratio $\xi_j = 0.5\%$ (light) and $\xi_j = 5.0\%$ (dark), with $\varsigma = 0$ (dashed) and $\varsigma = 0.2$ (solid) in Eq. (26): (a) $0 \le \omega_h/\omega_j \le 4$; (b) zoom $0.7 \le \omega_h/\omega_j \le 1.3$; (c) zoom $0 \le \omega_h/\omega_j \le 1$; and (d) zoom $1 \le \omega_h/\omega_j \le 4$.

predictions that only consider the resonant contribution, the following observations are made.

- As expected, considering only the resonant contribution allows for a good approximation of $\sigma_{\ddot{u}}$ for $\omega_h/\omega_j \simeq 1$. However, the accuracy of this approximation decreases for increasing modal damping ratios. For high modal damping ratios, Eq. (20) consistently results in an overestimation of $\sigma_{\ddot{u}}$. For modal damping ratios of 2% and 10%, Eq. (20) results in an overestimation of approximately 7% and 36%, respectively. In view of engineering applications, this (mild) overestimation is considered acceptable.
- Figs. 6(b and c) show that when only the resonant contribution is accounted for, the structural response is underestimated the further ω_h is from ω_j. Although these results show that for very low damping ratios the nonresonant response is low in comparison with the maximum resonant response, its (relative) importance increases for increasing modal damping ratios. Furthermore, the significance of nonresonant contributions will also increase when multiple modes contribute to the overall structural response.
- Fig. 6 shows that Krenk provides an excellent approximation of the standard deviation of the response for resonant conditions ($\omega_h/\omega_j \approx 1$), whereas it overestimates the standard deviation in other cases. The results in this figure correspond to a COV of the step frequency $c_s = 0.09$. Tubino and Piccardo (2016) showed that the quality of Krenk's approximation decreases for decreasing coefficients of variation.
- In addition, the following observations are made which are directly related to the dynamic behavior of a SDOF system:
  - as ω_h is further away from ω_j, the structural response becomes independent of the modal damping ratio;
  - for $\omega_h/\omega_j \ll 1$, the structural response converges to the quasi-static response, and therefore, the structural acceleration response converges to zero;
  - for $\omega_h/\omega_j \gg 1$, the structural response converges to a value which is inversely proportional to the modal mass.
- Finally, it is observed in Fig. 6 that the methodology proposed here in Eqs. (27), (19), (20), and (26), allows one to arrive at a good (and mildly conservative) estimate of $\sigma_{\ddot{u}}$ for any ω_h/ω_j.

Third, focus is on the two corrections for the nonresonant contribution proposed in section "Multiharmonic Excitation, Multimode Response." Fig. 7 visualizes the influence of evaluating the FRF $H_{\ddot{z}_j}(\omega)$ at a frequency ω'_h that is 20% ($\varsigma = 0.2$) closer to ω_j than ω_h [see also Eq. (26)]. Figs. 7(a and c) show that if $\varsigma = 0$ and, thus, the FRF $H_{\ddot{z}_j}(\omega)$ is evaluated at ω_h, the nonresonant contribution is underestimated slightly. Considering $\varsigma = 0.2$ allows one to arrive at a good and mildly conservative estimate of the nonresonant contribution. In turn, Fig. 8 visualizes the influence of the term $\mathbb{W}_j(\omega_h)$ [Eq. (26)] that enforces that there is no contribution of the nonresonant response at $\omega_h = \omega_j$ and that the influence of the nonresonant response gradually increases as ω_h moves further away from ω_j. Fig. 8 shows that if instead of $\mathbb{W}_j(\omega_h)$ the Heaviside function is used [see Eq. (23)], an unnatural jump is observed in the estimated standard deviation at the borders of the interval $[\omega_j - \varepsilon;\ \omega_j + \varepsilon]$. In this example ε is set to $0.1\omega_j$. Regardless of the value of ε, the unnatural jump remains and is associated with a region where the structural response is overestimated (when $\varepsilon/\omega_j \approx 1$) or underestimated (when $\varepsilon/\omega_j \ll 1$). Fig. 8 shows that this can be avoided by the use of a proper smooth alternative of the Heaviside function, as proposed in Eq. (26) by means of $\mathbb{W}_j(\omega_h)$.

Numerical Verification: Multiharmonic, Multimode

In this section, the proposed approach is challenged by means of its application to a real footbridge, the Eeklo footbridge (Fig. 9), where multiple modes contribute to the overall structural response. In addition, by considering different load cases, its performance is evaluated for load scenarios characterized by a different relative importance of resonant and nonresonant contributions. To facilitate interpretation, the results in this section are expressed in terms of frequency n (Hz) instead of circular frequency ω (rad/s).

The Eeklo footbridge is a lightweight steel footbridge with a central span of 42 m and two side spans of 27 m [Fig. 9(c)]. The bridge is simply supported with land abutments at the sides and two concrete piers

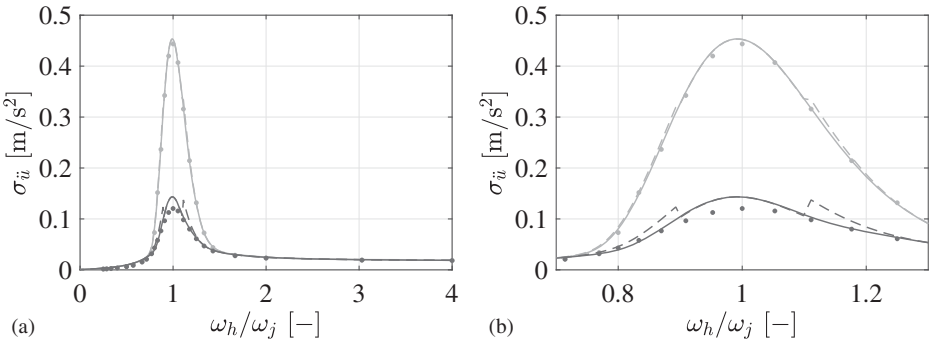

Fig. 8. Comparison between the analytically predicted (curve) and numerically simulated (•) standard deviation of $\ddot{u}$, in terms of ω_h/ω_j, for a pedestrian density of 0.5 pedestrians/m^2 and for a modal damping ratio $\xi_j = 0.5\%$ (light) and $\xi_j = 5.0\%$ (dark), according to Eq. (23) (dashed) and Eq. (26) (solid): (a) $0 \le \omega_h/\omega_j \le 4$; and (b) zoom $0.7 \le \omega_h/\omega_j \le 1.3$.

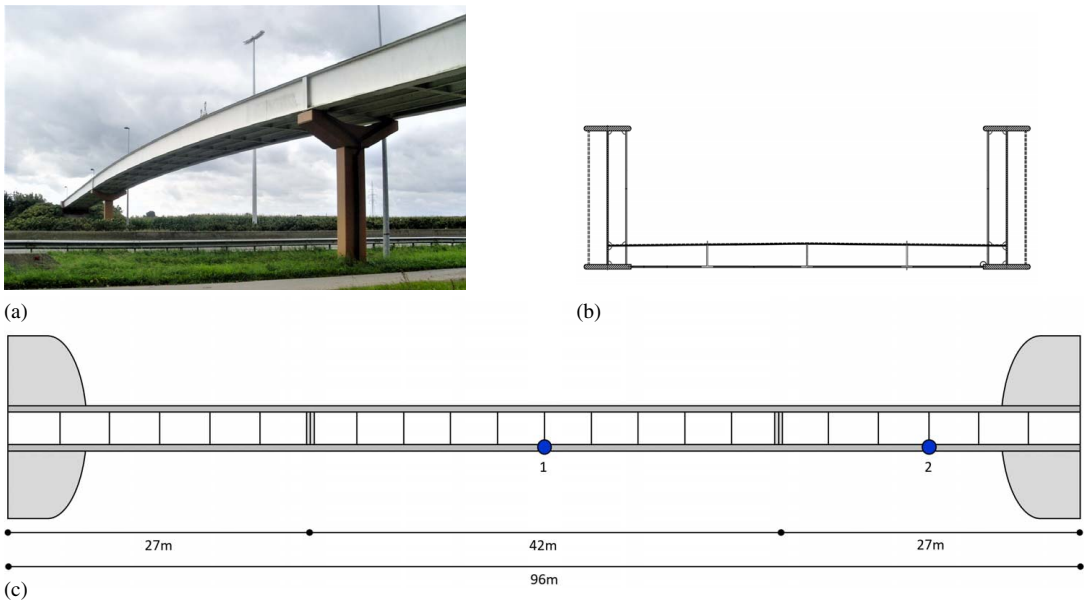

Fig. 9. (a) The Eeklo footbridge (image by K. Van Nimmen) with (b) cross section; and (c) plan view with the selected output locations at the center of the central span (1) and the side span (2).

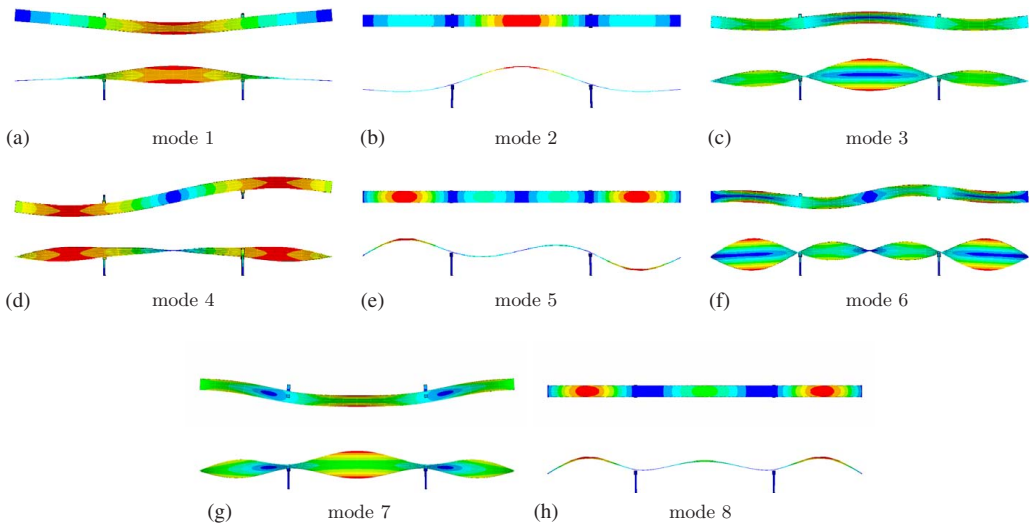

Fig. 10. Natural frequency, top and side view of mode 1 up to mode 8 of the Eeklo footbridge: (a) mode 1, 1.71 Hz, lateral-torsional; (b) mode 2, 3.02 Hz, vertical bending; (c) mode 3, 3.30 Hz, torsional; (d) mode 4, 3.43 Hz, lateral-torsional; (e) mode 5, 5.75 Hz, vertical bending; (f) mode 6, 5.80 Hz, lateral-torsional; (g) mode 7, 6.10 Hz, lateral-torsional; and (h) mode 8, 6.47 Hz, vertical bending.

at the center span. The cross section of the bridge [Fig. 9(b)] consists of two main beams with a height of 1.2 m at a spacing of 3.4 m. The total bridge mass (121 t) is composed of 95 t for the bridge deck and 26 t for the concrete pillars. The reader is referred to Van Nimmen et al. (2014) more information on the structural and dynamic characteristics of the Eeklo footbridge. In this application, the first eight modes are accounted for. The corresponding natural frequencies and mode shapes are presented in Fig. 10. For illustration purposes, a modal damping ratio of 0.5% is assumed for all modes.

The same pedestrian density, walking speed, and Gaussian distribution of step frequencies are considered as in section "Numerical Verification: Single-Harmonic, Single-Mode": a pedestrian density of 0.5 persons/m^2, corresponding to a total of $m_p = 136$ pedestrians on the footbridge, a walking speed $\bar{v}_s$ of 1.30 m/s and a standard deviation of $\sigma_{n_s} = 0.18$ Hz on the step frequencies. For illustration purposes, different values are considered for the mean value of the step frequencies $\bar{n}_s$, as discussed in the following paragraphs. The weight of the pedestrians is set to $\bar{G} = 700$ N (AFGC 2006; Walpole et al. 2012). The walking load is composed of two harmonics, with $\bar{\alpha}_1 = 0.4$ and $\bar{\alpha}_2 = 0.1$ (AFGC 2006).

For each case, the PSD function of the modal loads and the standard deviation of the structural dynamic response are estimated (1) numerically based on a large number of $m_{\text{sim}} = 10^4$ MC simulations (as described in section "Structural Response to Unrestricted

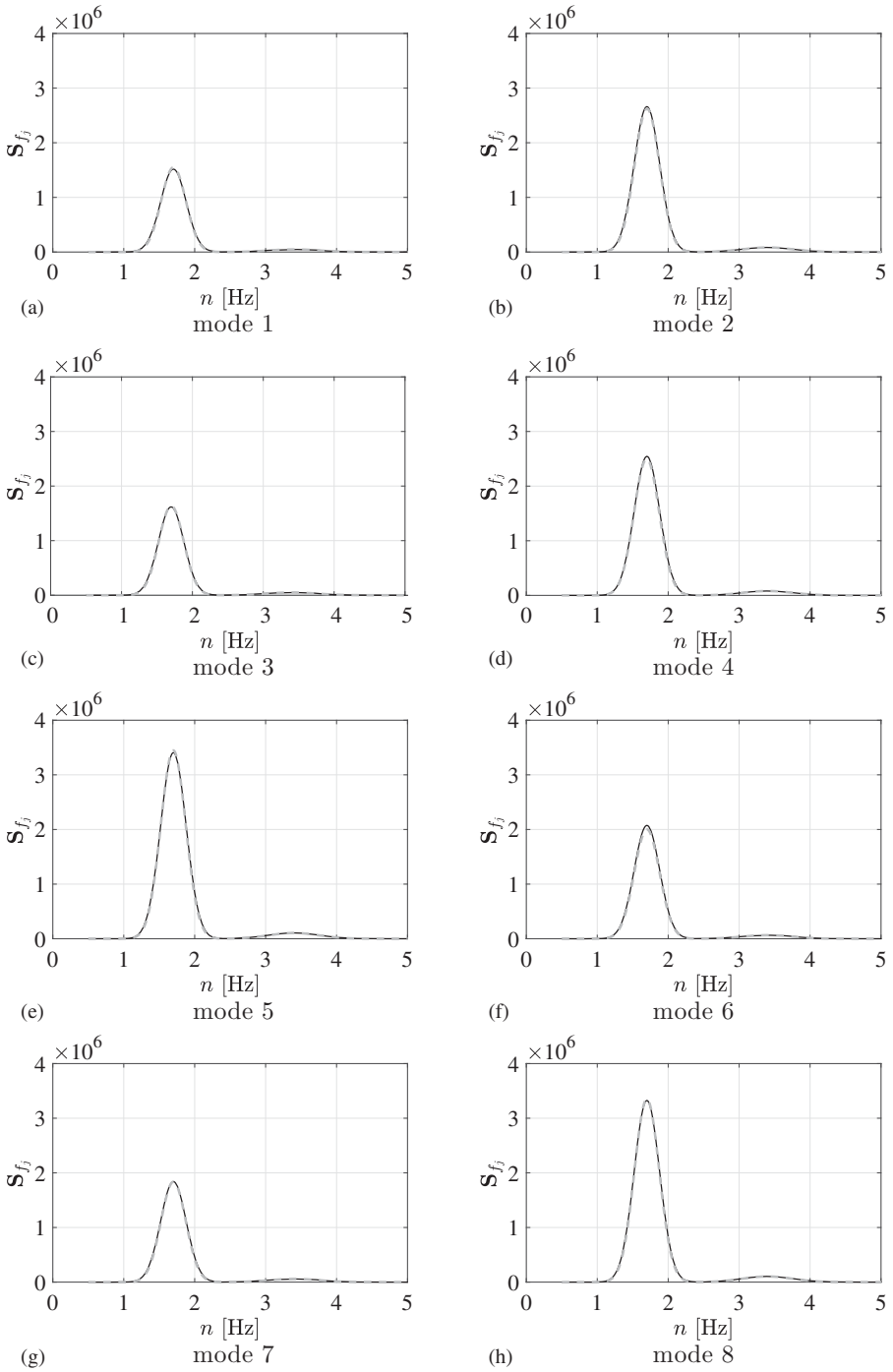

Fig. 11. PSD function of the modal force ($m_p = 136$) analytically predicted (solid, black) and numerically simulated (dashed, gray) for (a–h) modes 1–8 of the Eeklo footbridge, for $\bar{n}_s = 1.7$ Hz.

Pedestrian Traffic") and (2) by the simplified expressions proposed in section "Spectral Approach": Eq. (16) for the modal load and Eqs. (27), (19), (20), and (26) for the estimation of the dynamic response. As for the present application also torsional mode shapes are involved, the distribution of the pedestrians along the width of the bridge deck is relevant as well. To address this issue, straight walking trajectories are considered, with the lateral position of the pedestrians y randomly distributed along the width of the bridge deck l_y.

PSD Function of the Modal Load

Fig. 11 compares the PSD function of the modal load as predicted analytically by Eq. (16) and as derived from the MC simulations for the case where $\bar{n}_s = 1.7$ Hz. The following observations are made.

- The different modal loads are of the same order of magnitude. (Small) Differences arise due to the nature of the mode shape, where smaller amplitudes are found for torsional modes.
- For all modes, the contribution of the fundamental and the second harmonic of the walking load to the modal load can be clearly recognized. In addition, it is observed that the peak amplitude near $\bar{n}_s = 1.7$ Hz is $2 \times 16 = 2 \times (\bar{\alpha}_1/\bar{\alpha}_2)^2$ times larger than that near $2 \times \bar{n}_s = 3.4$ Hz, where the factor of 2 stems from $p_{1\omega_s}(\omega) = 2p_{2\omega_s}(2\omega)$ and, thus, $p_{1n_s}(n) = 2p_{2n_s}(2n)$.
- Excellent agreement is obtained between the analytically predicted and the numerically simulated PSD function of the modal load.

Structural Dynamic Response

Different values are assumed for the mean value of the step frequencies: $\bar{n}_s = [1.3, 2.3]$ Hz, in all cases with $\sigma_{n_s} = 0.18$ Hz. The output is evaluated at two locations: at the center of the central span and the side span, in both cases at the side of the parapet,

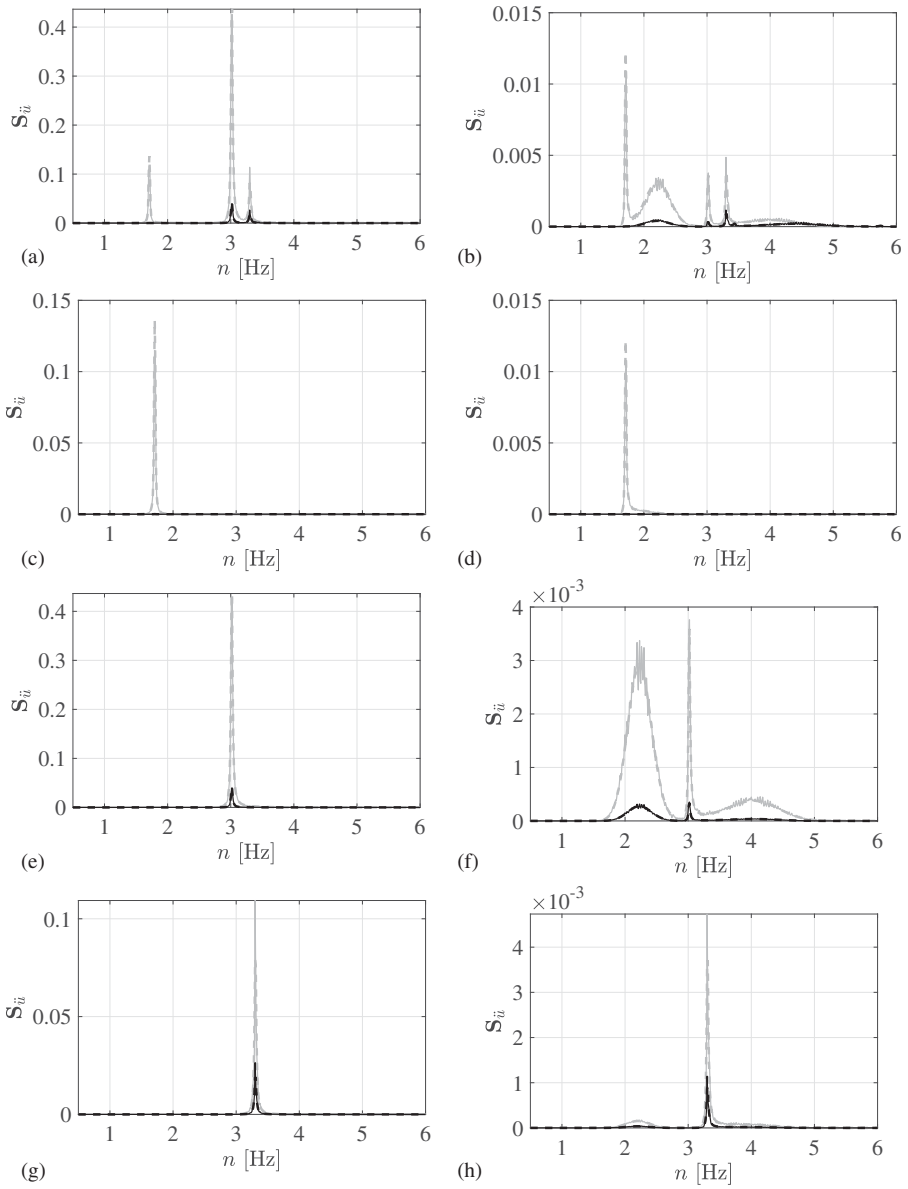

Fig. 12. The PSD function of structural accelerations at the central span (gray) and at the side span (black), numerically simulated (solid) and analytically predicted (dashed), for (a) $\bar{n}_s = 1.7$ Hz; (b) $\bar{n}_s = 2.1$ Hz; and the corresponding modal contributions of (c and d) mode 1; (e and f) mode 2; and (g and h) mode 3.

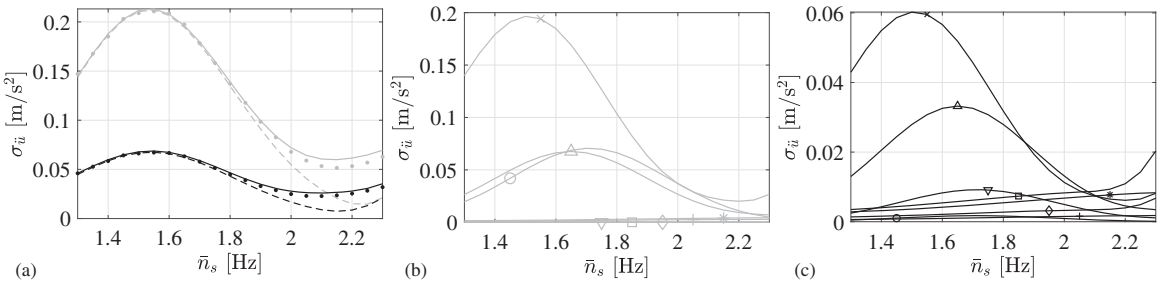

Fig. 13. The standard deviation of $\ddot{u}$ at the central span (gray) and at the side span (black), in terms of $\bar{n}_s$, for a pedestrian density of 0.5 pedestrians/m^2: (a) numerically simulated (•) and analytically predicted using only the resonant contribution (dashed) and both the resonant and nonresonant contribution (solid); and (b, c) the contribution of mode 1 (°), mode 2 (×), mode 3 (△), mode 4 (▽), mode 5 (), mode 6 (⋄), mode 7 (+), and mode 8 (*) at the central (b) and side (c) span.

implying contributions of both bending and torsional modes [Fig. 9(c)].

Figs. 12(a and b) present the PSD function of the structural acceleration levels at the central and side span, for the case where $\bar{n}_s = 1.7$ and $\bar{n}_s = 2.1$ Hz, respectively. Figs. 12(c) up to 12(h) present the corresponding modal contributions of the first three modes. The comparison is made between the analytical predictions [cf., Eqs. (9) and (17)] and the numerical simulations. The following observations are made.

- For $\bar{n}_s = 1.7$ Hz [Fig. 12(a)], the PSD function of the structural response at the central span is clearly characterized by the resonant response of mode 1, 2, and 3, whereas the PSD function of the structural response at the side span is clearly characterized by the resonant response of mode 2 and 3.
- For $\bar{n}_s = 2.1$ Hz [Fig. 12(b)], the PSD function of the structural response at the central span and side span is clearly characterized by the resonant response of mode 1, 2, and 3, as well as by nonnegligible nonresonant contributions around the fundamental (2.1 Hz) and second (4.2 Hz) harmonic of the walking load.
- For $\bar{n}_s = 2.1$ Hz, the modal contributions partially overlap [Figs. 12(d, f, and h)].
- There is a very good agreement between the numerically simulated and the analytical predicted PSD function of the structural acceleration levels.

Fig. 13(a) compares the standard deviation of the structural accelerations at the central and the side span in terms of the considered mean value for the step frequencies, as analytically predicted and derived from the numerical simulations for the range $\bar{n}_s = [1.3, 2.3]$ Hz. The analytical predictions are made (1) considering the resonant contributions only [Eq. (20)] and (2) considering both the resonant and nonresonant contributions [Eqs. (27), (19), (20), and (26)]. Fig. 13(b) presents the corresponding modal contributions. When in Fig. 13(a) the numerical simulations are compared with the analytical predictions based on the resonant contributions only, the following observations are made.

- For $1.3 < \bar{n}_s < 1.8$ Hz, excellent agreement is found between the analytical predictions and the values obtained from the numerical simulations. In this range, the resonant contributions dominate the structural response.
- For $1.8 < \bar{n}_s < 2.3$ Hz, the analytical predictions underestimate the structural response. In this case, the nonresonant contributions that are not accounted for in the analytical formulation contribute significantly to the overall structural response.

Fig. 13(b) shows that the structural response is mainly governed by the contributions of mode 1, 2, and 3 (at midspan) and mode 2 and 3 (at sidespan). Fig. 13(a) finally shows that, even though the response of the different modes partially overlap, the proposed spectral approach involving the SRSS combination rule allows for a very good (and mildly conservative) estimate of the standard deviation of the structural response by considering both resonant and nonresonant contributions.

Conclusions

In this work, a spectral load model available in the literature for unrestricted pedestrian traffic is extended to account for the multiple harmonics of the walking load and for its application to arbitrary mode shapes. Furthermore, a closed-form expression is proposed to estimate the variance of the structural response taking into account both resonant and nonresonant contributions. The proposed method furthermore allows the contribution of multiple modes to be accounted for, on the condition that the modes are widely spaced. This is a limitation that is met by the majority of footbridges. Every step in the generalization process is verified numerically using MC simulations, considering the variability of the relevant load parameters. The numerical verification process first considers the special case of single-harmonic excitation and single-mode structural dynamic response. The results show that when the mean value of the step frequencies is close to the natural frequency of the mode, the resonant contribution provides a very good estimate of the dynamic response. When this is not the case, the nonresonant contribution becomes important as well, and its relevance increases for increasing damping ratios. The results also show that the proposed closed-form expression provides a very accurate estimate of the total dynamic response. Next, the proposed approach is verified for the prediction of a multiharmonic excitation and multimode structural dynamic response, through the application to a real footbridge with eight modes with a natural frequency between 1.5 and 6.5 Hz. The results show that, for all modes, a perfect agreement is obtained for the PSD function of the modal load. Furthermore, the results show that the structural response is governed by resonant and nonresonant contributions of multiple modes. Finally, it is shown that, for all relevant load cases, the proposed methodology allows one to arrive at a good and mildly conservative estimate of the total structural dynamic response. Further research could involve experimental validation of the spectral approach, the proposal of a suitable combination rule to take into account modal correlation for closely spaced modes, and the extension and verification of the spectral load model to account for HHI.

Data Availability Statement

Some or all data, models, or code generated or used during the study are available from the corresponding author by request

(available data: Matlab® code to reproduce the results in the sections involving "Numerical Verification").

Acknowledgments

The first author is a postdoctoral fellow of the Research Foundation Flanders (FWO, 12E0816N). The research presented in this paper was performed within the framework of a research stay at the University of Genoa (FWO, Travel Grant V404918N). The financial support is gratefully acknowledged.

Notation

The following symbols are used in this paper:

c_h = coefficient of variation of α_h G;
c_s = coefficient of variation of the step frequency;
f, f_j = external force and jth modal force;
G = mean value of the weight of the pedestrians;
G_p = weight of the pth pedestrian;
h = index number of the harmonic component of the walking load;
$H_{\ddot{z}_j}$ = FRF of the jth modal coordinate in terms of accelerations;
j = index number of the mode;
l_x = dimension of the bridge deck along the longitudinal axis (length);
l_y = dimension of the bridge deck along the lateral axis (width);
m_h = number of harmonic components in the walking load;
m_j = jth modal mass;
m_m = number of modes;
m_p = number of pedestrians;
n_j = jth natural frequency;
p = index number of the pedestrian;
p_{ω_s} = PDF of the step frequency;
S_{f_j} = PSD function of the jth modal force;
$S_{f_{j,h}}$ = PSD function of the jth modal force associated with the hth harmonic;
$S_{\ddot{z}_j}$ = PSD function of the jth modal accelerations;
$u, \ddot{u}$ = displacement and acceleration of the footbridge;
$\bar{v}_s$ = mean value of the walking speed of the pedestrians;
x = abscissa along the longitudinal axis of the bridge deck;
x_p = abscissa along the longitudinal axis of the bridge deck of the pth pedestrian;
y = abscissa along the lateral axis of the bridge deck;
y_p = abscissa along the lateral axis of the bridge deck of the pth pedestrian;
z_j = jth modal coordinate;
$\bar{\alpha}_h$ = mean value of the DLF of the hth harmonic of the walking load;
α_{hp} = DLF of the hth harmonic of the walking load of the pth pedestrian;
ω_h = mean value of the hth harmonic of the circular step frequency;
ω_j = jth natural circular frequency;
ω_s = circular step frequency;
$\bar{\omega}_s$ = mean value of the circular step frequency; and
ω_{sp} = circular step frequency of the pth pedestrian.
ϕ_j = jth unity-normalized mode shape;
σ_{ω_s} = standard deviation of the circular step frequency;
$\sigma_{\ddot{u}}$ = standard deviation of the acceleration response;
$\sigma_{\ddot{z}_j}$ = standard deviation of the acceleration of the jth modal coordinate;
$\sigma_{\ddot{z}_{j,R}}$ = resonant contribution to the standard deviation of the acceleration of the jth modal coordinate;
$\sigma_{\ddot{z}_{j,\mathrm{NR}}}$ = nonresonant contribution to the standard deviation of the acceleration of the jth modal coordinate;
τ_p = arrival time of the pth pedestrian;
θ_h = phase angle of the hth harmonic;
θ_p = phase angle of the pth pedestrian; and
ξ_j = jth modal damping ratio.

References

AFGC (Association Française de Génie Civil, Sétra). 2006. *Sétra: Evaluation du comportement vibratoire des passerelles piétonnes sous l'action des piétons (Assessment of vibrational behaviour of footbridges under pedestrian loading)*. Paris: AFGC.

Agu, E., and M. Kasperski. 2011. "Influence of the random dynamic parameters of the human body on the dynamic characteristics of the coupled system structure-crowd." *J. Sound Vib.* 330 (3): 431–444. https://doi.org/10.1016/j.jsv.2010.06.029.

Bassoli, E., K. Van Nimmen, L. Vincenzi, P. Van den Broeck. 2018. "A spectral load model for pedestrian excutation including vertical human-structure interaction." *Eng. Struct.* 156: 537–547. https://doi.org/10.1016/j.engstruct.2017.11.050.

Bendat, J., and A. Piersol. 2010. *Random data: Analysis and measurement procedures*. Hoboken, NJ: John Wiley & Sons.

Bocian, M., J. Burn, J. MacDonald, and J. Brownjohn. 2016. "From phase drift to synchronisation – pedestrian stepping behaviour on laterally oscillating structures and consequences for dynamic stability." *J. Sound Vib.* 392: 382–399. https://doi.org/10.1016/j.jsv.2016.12.022.

Bocian, M., J. H. G. Macdonald, and J. F. Burn. 2012. "Biomechanically inspired modelling of pedestrian-induced forces on laterally oscillating structures." *J. Sound Vib.* 331 (16): 3914–3929. https://doi.org/10.1016/j.jsv.2012.03.023.

Brownjohn, J. M. W., A. Pavić, and P. Omenzetter. 2004. "A spectral density approach for modelling continuous vertical forces on pedestrian structures due to walking." *Can. J. Civ. Eng.* 31 (1): 65–77. https://doi.org/10.1139/l03-072.

Bruno, L., and A. Corbetta. 2017. "Uncertainties in crowd dynamic loading of footbridges: A novel multi-scale model of pedestrian traffic." *Eng. Struct.* 147: 545–566. https://doi.org/10.1016/j.engstruct.2017.05.066.

Bruno, L., A. Corbetta, and A. Tosin. 2016. "From individual behaviour to an evaluation of the collective evolution of crowds along footbridges." *J. Eng. Math.* 101 (1): 153–173. https://doi.org/10.1007/s10665-016-9852-z.

Bruno, L., A. Tosin, P. Tricerri, and F. Venuti. 2011. "Non-local first-order modelling of crowd dynamics: A multidimensional framework with applications." *Appl. Math. Modell.* 35 (1): 426–445. https://doi.org/10.1016/j.apm.2010.07.007.

Bruno, L., and F. Venuti. 2009. "Crowd-structure interaction in footbridges: Modelling, application to real case-study and sensitivity analysis." *J. Sound Vib.* 323 (1–2): 475–493. https://doi.org/10.1016/j.jsv.2008.12.015.

BSI (British Standards Institution). 2008. *UK National Annex to Eurocode 1. Actions on structures. Traffic loads on bridges*. London: BSI.

Butz, C., M. Feldmann, C. Heinemeyer, and G. Sedlacek. 2008. *SYNPEX: Advanced load models for synchronous pedestrian excitation and optimised design guidelines for steel footbridges*. Technical Rep. No. RFCSResearch Project RFS-CR-03019. Research Fund for Coal and Steel. Luxembourg: Office for Official Publications of the European Communities.

Cappellini, A., S. Manzoni, M. Vanali, and A. Cigada. 2016. "Evaluation of the dynamic behaviour of steel staircases damped by the presence of people." *Eng. Struct.* 115: 165–178. https://doi.org/10.1016/j.engstruct.2016.02.028.

Caprani, C. C. 2014. "Application of the pseudo-excitation method to assessment of walking variability on footbridge vibration." *Comput. Struct.* 132: 43–54. https://doi.org/10.1016/j.compstruc.2013.11.001.

Caprani, C., and E. Ahmadi. 2016. "Formulation of human–structure interaction system models for vertical vibration." *J. Sound Vib.* 377: 346–367. https://doi.org/10.1016/j.jsv.2016.05.015.
Caprani, C. C., J. Keogh, P. Archbold, and P. Fanning. 2012. "Enhancement for the vertical response of footbridges subjected to stochastic crowd loading." *Comput. Struct.* 102–103: 87–96. https://doi.org/10.1016/j.compstruc.2012.03.006.
Carroll, S. P., J. S. Owen, and M. F. M. Hussein. 2012. "Modelling crowd-bridge dynamic interaction with a discrete defined crowd." *J. Sound Vib.* 331 (11): 2685–2709. https://doi.org/10.1016/j.jsv.2012.01.025.
Carroll, S. P., J. S. Owen, and M. F. M. Hussein. 2014. "Experimental identification of the lateral human-structure interaction mechanism and assessment of the inverted-pendulum biomechanical model." *J. Sound Vib.* 333 (22). 5865–5884. https://doi.org/10.1016/j.jsv.2014.06.022.
Casciati, F., S. Casciati, and L. Faravelli. 2017. "A contribution to the modelling of human induced excitation on pedestrian bridges." *Struct. Saftey* 66: 51–61. https://doi.org/10.1016/j.strusafe.2017.01.004.
Chen, J., J. Wang, and J. Brownjohn. 2019. "Power spectral density model for pedestrian walking load." *J. Struct. Eng.* 145 (2): 04018239. https://doi.org/10.1061/(ASCE)ST.1943-541X.0002248.
Chopra, A. K. 1995. *Dynamics of structures: Theory and applications to earthquake engineering*. Upper Saddle River, NJ: Prentice Hall.
Dallard, P., T. Fitzpatrick, A. Flint, A. Low, R. Smith, M. Willford, and M. Roche. 2001. "The London millennium footbridge: Pedestrian-induced lateral vibration." *J. Bridge Eng.* 6 (6): 412–417. https://doi.org/10.1061/(ASCE)1084-0702(2001)6:6(412).
Dang, H., and S. Živanović. 2016. "Influence of low-frequency vertical vibration on walking locomotion." *J. Struct. Eng.* 142 (12): 1–12. https://doi.org/10.1016/j.engstruct.2016.04.007.
Davenport, A. G. 1964. "Note on the distribution of the largest value of a random function with application to gust loading." *Proc. Inst. Civ. Eng.* 28: 187–196.
Demartino, C., A. Avossa, and F. Ricciardelli. 2017. "Deterministic and probabilistic serviceability assessment of footbridge vibrations due to a single walker crossing." *Shock Vib.* 2018 (1917629): 1–26.
Dey, P., A. Sychterz, S. Narasimhan, and S. Walbridge. 2016. "Performance of pedestrian-load models through experimental studies on lightweight aluminium bridges." *J. Bridge Eng.* 21 (8): C4015005. https://doi.org/10.1061/(ASCE)BE.1943-5592.0000824.
Elishakoff, I. 1999. *Probabilistic theory of structures*. 2nd ed. Mineola, NY: Dover.
Erlicher, S., A. Trovato, and P. Argoul. 2010. "Modelling the lateral pedestrian force on a rigid floor by a self-sustained oscillator." *Mech. Syst. Sig. Process.* 24 (5): 1579–1604. https://doi.org/10.1016/j.ymssp.2009.11.006.
Ferrarotti, A., and F. Tubino. 2016. "Generalized equivalent spectral model for vibration serviceability analysis for footbridges." *J. Bridge Eng.* 21 (12): 04016091. https://doi.org/10.1061/(ASCE)BE.1943-5592.0000963.
Fujino, Y., and D. Siringoringo. 2015. "A conceptual review of pedestrian-induced lateral vibration and crowd synchronization problem on footbridges." *J. Bridge Eng.* 21 (8): 1–12.
Goodman, L. 1960. "On the exact variance of products." *J. Am. Stat. Assoc.* 55 (292): 708–713. https://doi.org/10.1080/01621459.1960.10483369.
Heinemeyer, C., et al. 2009a. *Design of Lightweight Footbridges for Human Induced Vibrations - Background document in support to the implementation, harmonization and further development of the Eurocodes*. JRC-ECCS 2009. Luxembourg: Office for Official Publications of the European Communities.
Heinemeyer, C., et al. 2009b. *Design of Lightweight Footbridges for Human Induced Vibrations - Background document in support to the implementation, harmonization and further development of the Eurocodes*. Technical Rep., JRC-ECCS Scientific and Technical Reports. Brussels, Belgium: European Commission.
Helbing, D., I. Farkas, and T. Vicsek. 2000. "Simulating dynamical features of escape panic." *Nature* 407 (6803): 487–490. https://doi.org/10.1038/35035023.
Helbing, D., and P. Molnar. 1995. "Social force model for pedestrian dynamics." *Phys. Rev.* 51 (5): 4282–4286.
Ingólfsson, E. T., C. T. Georgakis, and J. Jönsson. 2012. "Pedestrian-induced lateral vibrations of footbridges: A literature review." *Eng. Struct.* 45: 21–52. https://doi.org/10.1016/j.engstruct.2012.05.038.
Krenk, S. 2012. "Dynamic response to pedestrian loads with statistical frequency distribution." *J. Eng. Mech.* 138 (10): 1275–1281. https://doi.org/10.1061/(ASCE)EM.1943-7889.0000425.
McDonald, M., and S. Živanović. 2017. "Measuring ground reaction force and quantifying variability in jumping and bobbing actions." *J. Struct. Eng.* 143 (2): 04016161. https://doi.org/10.1061/(ASCE)ST.1943-541X.0001649.
Ney, L., and C. Poulissen. 2014. "Design - An integrated approach." In *Proc., 5th Int. Footbridge Conf.*, edited by L. Debell and H. Russel, 96–99. London, UK: Hemming Information Services.
Pedersen, L., and C. Frier. 2010. "Sensitivity of footbridge vibrations to stochastic walking parameters." *J. Sound Vib.* 329 (13): 2683–2701. https://doi.org/10.1016/j.jsv.2009.12.022.
Piccardo, G., and F. Tubino. 2012. "Equivalent spectral model and maximum dynamic response for the serviceability analysis of footbridges." *Eng. Struct.* 40: 445–456. https://doi.org/10.1016/j.engstruct.2012.03.005.
Pizzimenti, A. D., and F. Ricciardelli. 2005. "Experimental evaluation of the dynamic lateral loading of footbridges by walking pedestrians." In *Proc., 6th European Conf. on Structural Dynamics*, 435–440. Rotterdam, Netherlands: Millpress Science.
Racić, V., and J. Brownjohn. 2011. "Stochastic model of near-periodic vertical loads due to humans walking." *Adv. Eng. Inf.* 25 (2): 259–275. https://doi.org/10.1016/j.aei.2010.07.004.
Racić, V., A. Pavić, and P. Reynolds. 2009. "Experimental identification and analytical modelling of walking forces: A literature review." *J. Sound Vib.* 326 (1–2): 1–49. https://doi.org/10.1016/j.jsv.2009.04.020.
Ricciardelli, F., and A. Pizzimenti. 2007. "Lateral walking-induced forces on footbridges." *J. Bridge Eng.* 12 (6): 677–688. https://doi.org/10.1061/(ASCE)1084-0702(2007)12:6(677).
Sachse, R., A. Pavić, and P. Reynolds. 2004. "Parametric study of modal properties of damped two-degree-of-freedom crowd-structure dynamic systems." *J. Sound Vib.* 274 (3–5): 461–480. https://doi.org/10.1016/j.jsv.2003.08.052.
Sahnaci, C., and M. Kasperski. 2005. "Random loads induced by walking." In *Proc., 6th European Conf. on Structural Dynamics*, 441–446. Rotterdam, Netherlands: Millpress Science.
Sahnaci, C., and M. Kasperski. 2011. "Simulation of random pedestrian flow." In *Proc., 8th European Conf. on Structural Dynamics*, edited by G. De Roeck, G. Degrande, G. Lombaert, G. Muller, 1040–1047. Leuven, Belgium: Katholieke Universiteit Leuven.
Shahabpoor, E., A. Pavić, and V. Racić. 2016a. "Identification of mass-spring-damper model of walking humans." *Structures* 5: 233–246. https://doi.org/10.1016/j.istruc.2015.12.001.
Shahabpoor, E., A. Pavić, and V. Racić. 2016b. "Interaction between walking humans and structures in vertical direction : A literature review." *Shock Vib.* 2016: 1–22.
Smith, A., S. Hicks, and P. Devine. 2009. *Design of floors for vibration: A new approach*. Revised ed. Ascot, UK: Steel Construction Institute.
Tubino, F. 2018. "Probabilistic assessment of the dynamic interaction between multiple pedestrians and vertical vibrations of footbridges." *J. Sound Vib.* 417: 80–96. https://doi.org/10.1016/j.jsv.2017.11.057.
Tubino, F., L. Carassale, and G. Piccardo. 2016. "Human-induced vibrations on two lively footbridges in Milan." *J. Bridge Eng.* 21 (8): C4015002. https://doi.org/10.1061/(ASCE)BE.1943-5592.0000816.
Tubino, F., and G. Piccardo. 2016. "Serviceability assessment of footbridges in unrestricted pedestrian traffic conditions." *Struct. Infrastruct. Eng.* 12 (12): 1650–1660. https://doi.org/10.1080/15732479.2016.1157610.
Van Nimmen, K., G. Lombaert, G. De Roeck, and P. Van den Broeck. 2017. "The impact of vertical human-structure interaction on the response of footbridges to pedestrian excitation." *J. Sound Vib.* 402: 104–121. https://doi.org/10.1016/j.jsv.2017.05.017.
Van Nimmen, K., G. Lombaert, I. Jonkers, G. De Roeck, and P. Van den Broeck. 2014. "Characterisation of walking loads by 3D inertial motion

tracking." *J. Sound Vib.* 333 (20): 5212–5226. https://doi.org/10.1016/j.jsv.2014.05.022.

Van Nimmen, K., P. Verbeke, G. Lombaert, G. De Roeck, and P. Van den Broeck. 2016. "Numerical and experimental evaluation of the dynamic performance of a footbridge with tuned mass dampers." *J. Bridge Eng.* 21 (8): C4016001. https://doi.org/10.1061/(ASCE)BE.1943-5592.0000815.

Venuti, F., and L. Bruno. 2007. "An interpretative model of the pedestrian fundamental relation." *C. R. Mec.* 335 (4): 194–200. https://doi.org/10.1016/j.crme.2007.03.008.

Venuti, F., V. Racić, and A. Corbetta. 2016. "Modelling framework for dynamic interaction between multiple pedestrians and vertical vibrations of footbridges." *J. Sound Vib.* 379: 245–263. https://doi.org/10.1016/j.jsv.2016.05.047.

Walpole, S. C., D. Prieto-Merino, P. Edwards, J. Cleland, G. Stevens, and I. Roberts. 2012. "The weight of nations: An estimation of adult human biomass." *BMC Public Health* 12 (1): 439. https://doi.org/10.1186/1471-2458-12-439.

Weber, B., and G. Feltrin. 2010. "Assessment of long-term behavior of tuned mass dampers by system identification." *Eng. Struct.* 32 (11): 3670–3682. https://doi.org/10.1016/j.engstruct.2010.08.011.

Wei, X., P. Van den Broeck, G. De Roeck, and K. Van Nimmen. 2017. "A simplified method to account for the effect of human-human interaction on the pedestrian-induced vibrations of footbridges." In *Proc., 10th European Conf. on Structural Dynamics*, edited by F. Vestroni, F. Romeo, and V. Gattulli, 2907–2912. Elsevier: Procedia Engineering.

Weidmann, U. 1993. *Transporttechnik der fussganger (Transport technology of the pedestrian)*. Zurich, Switzerland: Schriftenreihe IVT-Berichte.

Willford, M., and P. Young. 2006. *A design guide for footfall induced vibration of structures*. Camberley Surrey: Concrete Center.

Živanović, S. 2012. "Benchmark footbridge for vibration serviceability assessment under vertical component of pedestrian load." *J. Struct. Eng.* 138 (10): 1193–1202. https://doi.org/10.1061/(ASCE)ST.1943-541X.0000571.

Živanović, S., A. Pavić, and E. Ingólfsson. 2010. "Modelling spatially unrestricted pedestrian traffic on footbridges." *J. Struct. Eng.* 136 (10): 1296–1308. https://doi.org/10.1061/(ASCE)ST.1943-541X.0000226.

Živanović, S., A. Pavić, and P. Reynolds. 2005. "Vibration serviceability of footbridges under human-induced excitation: A literature review." *J. Sound Vib.* 279 (1–2): 1–74.

Živanović, S., A. Pavić, and P. Reynolds. 2007. "Probability-based prediction of multi-mode vibration response to walking excitation." *Eng. Struct.* 29 (6): 942–954. https://doi.org/10.1016/j.engstruct.2006.07.004.